Progress In Electromagnetics Research, PIER 38, 283–310, 2002

SCATTERING BY AN ARRAY OF CONDUCTING, LOSSY DIELECTRIC, FERRITE AND PSEUDOCHIRAL CYLINDERS

M. Polewski and J. Mazur

Department of Electronics
Telecommunications and Informatics
Technical University of Gdańsk
ul. Narutowicza 11/12, 80-952 Gdańsk, Poland

Abstract—Theory of scattering by conducting, lossy dielectric, ferrite and/or pseudochiral cylinders is investigated using a combination of a modified iterative scattering procedure and the orthogonal expansion method. The addition theorems for vector cylindrical harmonics, which transform harmonics from one coordinate system to another, are presented. The scattered field patterns for open structures and frequency responses of the transmission coefficients in a rectangular waveguide describing the resonances of the posts on the dominant waveguide mode are derived. The validity and accuracy of the method is verified by comparing the numerical results with those given in literature.

1. INTRODUCTION

Considering the electromagnetic wave scattering from two-dimensional arbitrary obstacles we can observe two areas of active research. The first area concerns open problems — obstacles in free space, where the far scattered field patterns can be investigated [1–6], while the second — closed problems — presents the frequency responses of described structure in a rectangular waveguide [7–13].

For open structures, different techniques e.g. integral equation formulation, partial differential equation, hybrid techniques combining the partial differential equation method with the eigenfunction expansion method have been developed for plane wave and line source excitations [1–4]. In the last decade, a recursive algorithm has been developed for the scattering by arbitrarily shaped obstacles [5]. Elsherbeni *et al.* [6] proposed an iterative solution for the scattering by I different parallel circular cylinders. The scattered field from each obstacle has been transferred to infinity by far field approximations.

For closed problems authors distinguished an interior area, which can be matched with other external fields. A lot of methods have been applied to analyze closed structures. Nielsen in [7] used the modal expansion method. Sahalos and Vafiadis [8] presented multifilament current model and for the first time applied circular interaction region instead of rectangular used by Nielsen. The boundary- and finite-element methods have also been utilized in [9, 10]. Gesche and Löchel applied the orthogonal expansion method for one [11] and two [12] posts positioned in one cross section of a rectangular waveguide. Recently, Valero and Ferrando [13] presented the method, which segments the problem into regions that are characterized by their generalized admittance matrices.

The purpose of this paper is to develop the method, that allows to investigate both open and closed problems. To solve this, it is convenient to separate cylindrical interaction region ξ (see Fig. 1), on the surface of which, a total scattered field from all cylinders can be found. Presented approach forced modification of iterative scattering procedure [6], where excitations in form of plane wave or Gaussian beam were known, but they limited investigations to open structures.

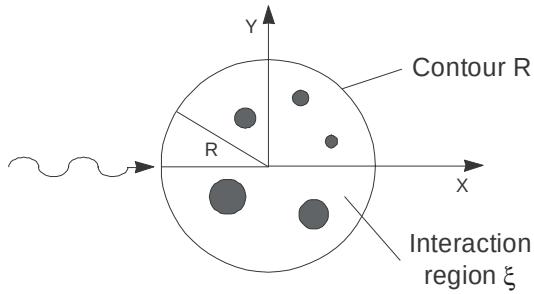

Figure 1. Cylindrical obstacles in the interaction region excited by E^z-wave.

The main difference between proposal method and the method in [6], is that the cylinders are excited by an unknown incident fields defined as an infinite series of Bessel functions of the first kind with an unknown coefficients a_n. These unknown coefficients a_n determine a total scattered field from all cylinders on a contour R. It allows to match it with other known incident fields and consequently to define scattering matrix of considering structure. In this case, presented approach allows to solve both scattering and waveguide problems. Proposed method has been developed to analyze scattering by conducting, lossy dielectric, ferrite and/or pseudochiral cylinders and can be applied to research a waveguide structures where incident fields are the TE_{n0} modes and open structures, to define scattered field patterns at any distance from investigating configurations of cylinders for E^z-wave excitation.

2. BASIC FORMULATION

2.1. Interaction Region

Consider harmonic E_z-wave excitation in global coordinates as infinite series of Bessel functions of the first kind with unknown coefficients a_n, where the electric field has a z component only with all vectors independent of z of the cylindrical coordinates (ρ, ϕ, z).

$$E_z^{inc(0)} = \sum_{n=-\infty}^{\infty} a_n J_n(k_0\rho) e^{jn\phi} \tag{1}$$

where k_0 is the wave number in free space.

Now it is assumed that field (1) excites number of I homogeneous, conducting, lossy dielectric, ferrite or pseudochiral cylinders (see

Fig. 1) and has to be defined in their local coordinates. For the i^{th} cylinder using an addition theorem for Bessel functions [14] one has

$$E_{zi}^{inc(0)} = \sum_{n=-\infty}^{\infty} a_n \sum_{m=-\infty}^{\infty} J_m(k_0 r_i) e^{jm\phi_i} J_{m-n}(k_0 d_{io}) e^{j(n-m)\phi_{io}} \quad (2)$$

where d_{io}, ϕ_{io} are defined in Fig. 2.

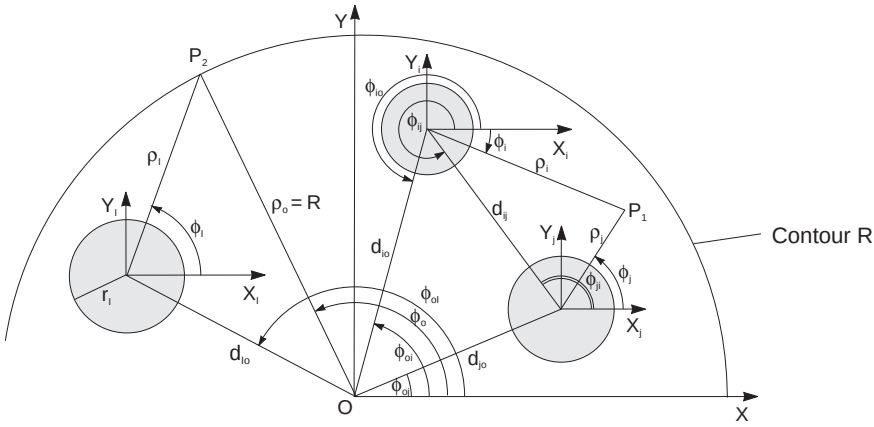

Figure 2. Notation used for a change of coordinate system for Bessel functions.

In response to our excitation, a zero order scattered field is created from each of I cylinders by forcing the tangential components of both the electric and magnetic fields, on the surface of each cylinder, to be continuous.

$$E_{zi}^{inc(0)}(r_i, \phi_i) + E_{zi}^{s(0)}(r_i, \phi_i) = E_{zi}^{d(0)}(r_i, \phi_i) \quad (3)$$

$$H_{\phi i}^{inc(0)}(r_i, \phi_i) + H_{\phi i}^{s(0)}(r_i, \phi_i) = H_{\phi i}^{d(0)}(r_i, \phi_i) \quad (4)$$

where r_i is the radius of the i^{th} cylinder.

The scattered electric field component for the i^{th} cylinder can be expressed as

$$E_{zi}^{s(0)}(\rho_i, \phi_i) = \sum_{n=-\infty}^{\infty} c_{in}^0 H_n^{(2)}(k_0 \rho_i) e^{jn\phi_i} \quad (5)$$

while transmitted field component inside the i^{th} cylinder is given by

$$E_{zi}^{d(0)}(\rho_i, \phi_i) = \sum_{n=-\infty}^{\infty} b_{in}^0 J_n(k_i \rho_i) e^{jn\phi_i} \quad (6)$$

where c_{in}^0 and b_{in}^0 are the unknown coefficients, $J_n(k_i\rho_i)$, $H_n^{(2)}(k_0\rho_i)$ denotes Bessel and Hankel functions respectively.
Applying (2) into (3) and (4), orthogonalizing by $e^{-jm\phi_i}$ and taking into account $n = N$ and $m = M$ harmonics the solution is obtained from the point of view of the unknown coefficients c_{in}^0 of the i^{th} cylinder.

$$[c_i^0] = [G_i] \cdot [T_{io}] \cdot [a] \tag{7}$$

where the forms of matrix $[G_i]$, H_ϕ and k_i for dielectric, ferrite and pseudochiral cylinder are given in Appendix.

Transformation of Bessel functions from global coordinates to the local coordinates of the i^{th} cylinder is expressed by matrix:

$$[T_{io}] = \left[J_{m-n}(k_0 d_{io}) e^{j(n-m)\phi_{io}}\right]_{m=-M,n=-N}^{M,N} \tag{8}$$

and m, n are rows and columns indexes respectively, while $[a]$ defines a vector

$$[a] = [\ a_{-M} \quad \ldots \quad a_{-1} \quad a_0 \quad a_1 \quad \ldots \quad a_M\ ]^T \tag{9}$$

In the next interaction, we use scattered fields from I-1 cylinders obtained in the previous interaction, as a new incident field on the i^{th} remaining cylinder.

$$E_{zi}^{inc(1)} = E_0 \sum_{\substack{j=1 \\ j\neq i}}^{I} \sum_{n=-\infty}^{\infty} c_{jn}^0 H_n^{(2)}(k_0\rho_j) e^{jn\phi_j} \tag{10}$$

To transfer the scattered fields from I-1 cylinders to the local coordinate of the i^{th} cylinder the Graf's addition theorem for Bessel functions is used [14].

$$H_n^{(2)}(k_0\rho_j)\, e^{jn\phi_j} = \begin{cases} \displaystyle\sum_{m=-\infty}^{\infty} H_{m-n}^{(2)}(k_0 d_{ij}) e^{j(n-m)\phi_{ij}} J_m(k_0\rho_i) e^{jm\phi_i} & \text{for } d_{ij} \geq \rho_i \\ \displaystyle\sum_{m=-\infty}^{\infty} J_{m-n}(k_0 d_{ij}) e^{j(n-m)\phi_{ij}} H_m^{(2)}(k_0\rho_i) e^{jm\phi_i} & \text{for } d_{ij} < \rho_i \end{cases} \tag{11}$$

In response to our new excitation, the first order ($p = 1$) scattered and transmitted field is created from each of I cylinders like in (5) and (6) but with new unknown coefficients c_{in}^1 and b_{in}^1. Using (3) and (4) with the first order fields the following solution is obtained.

$$\left[c_i^1\right] = [G_i] \sum_{\substack{j=1 \\ j\neq i}}^{I} \left[T_{ij}^H\right] \cdot \left[c_j^0\right] \tag{12}$$

where

$$\left[T_{ij}^{H}\right] = \left[H_{m-n}^{(2)}(k_0 d_{ij})e^{j(n-m)\phi_{ij}}\right]_{m=-M,n=-N}^{M,N}$$

and m, n are rows and columns indexes respectively. The matrix $[T_{ij}^{H}]$ provides transformation of Hankel functions of the second kind located in the coordinates of the j^{th} cylinder to the ones located in the coordinates of the i^{th} cylinder.

This approach gives us a next order scattered field and repeated for each individual cylinder leads us to an iterative scattering procedure where the coefficients of the p^{th} interaction depend only on the coefficients of the $(p-1)^{th}$ interaction.

$$[C^p] = [T^{ij}] \cdot [C^{p-1}] \cdot [a] \tag{13}$$

where

$$[C^p] = \begin{bmatrix} [c_1^p] \\ \cdot \\ [c_i^p] \\ \cdot \\ [c_I^p] \end{bmatrix} \qquad \left[T^{ij}\right] = \begin{bmatrix} [0] & \cdot & [T_{1,j}] & \cdot & [T_{1,I}] \\ \cdot & [0] & \cdot & \cdot & \cdot \\ [T_{j,1}] & \cdot & \cdot & \cdot & [T_{j,I}] \\ \cdot & \cdot & [T_{i,j}] & [0] & \cdot \\ [T_{I,1}] & \cdot & [T_{I,j}] & \cdot & [0] \end{bmatrix}$$

for $p = 2, 3, \ldots$ and $[c_i^p]$, $[0]$, $[T_{i,j}]$ are square sub-matrices where

$$[T_{i,j}] = [G_i] \cdot \left[T_{ij}^{H}\right] \tag{14}$$

Iterative procedure gives us the scattered field from the i^{th} cylinder in its local coordinates as follows

$$[E_{zi}^{S}] = [H_i^{\rho}] \cdot [C_i] \cdot [a] \tag{15}$$

where

$$[C_i] = \sum_{p=0}^{P} [c_i^p], \; [H_i^{\rho}] = diag\left(H_m^{(2)}(k_0\rho_i)e^{jm\phi_i}\right)_{m=-M}^{M}$$

and P is the number of interactions.

Using transformation (11) for $d_{ij} < \rho_o$ the scattered field from each cylinder is transferred to global coordinate system. Therefore the scattered electric field from the i^{th} cylinder on the surface of the interaction region (see Fig. 2) is given as

$$[E_{zi}^{SG}] = [H_i^{R}] \cdot [T_{oi}^{G}] \cdot [C_i] \cdot [a] \tag{16}$$

where

$$\begin{aligned}[H_i^R] &= diag\left(H_m^{(2)}(k_0R)e^{jm\phi}\right)_{m=-M}^{M},\\ [T_{oi}^G] &= \left[J_{m-n}(k_0d_{oi})e^{j(n-m)\phi_{oi}}\right]_{m=-M,n=-N}^{M,N}\end{aligned}$$

and $m,\ n$ are rows and columns indexes respectively.

Writing (16) for electric and magnetic field for each of I cylinders the following matrix equations is obtained:

$$[E_z^{SG}] = [H^R]\cdot[T^G]\cdot[C]\cdot[a] \tag{17}$$

$$\left[H_\phi^{SG}\right] = \frac{1}{j\omega\mu_0}[H'^R]\cdot[T^G]\cdot[C]\cdot[a] \tag{18}$$

where

$$\begin{aligned}[E_z^{SG}] &= \left[[E_{z1}^{SG}]\,..\,[E_{zi}^{SG}]\,..\,[E_{zI}^{SG}]\right]^T,\\ [H_\phi^{SG}] &= \left[[H_{\phi1}^{SG}]\,..\,[H_{\phi i}^{SG}]\,..\,[H_{\phi I}^{SG}]\right]^T\end{aligned}$$

and

$$[H^R] = \begin{bmatrix} \left[H_1^R\right] & \cdot & [0] & \cdot & [0] \\ \cdot & \cdot & \cdot & \cdot & \cdot \\ [0] & \cdot & \left[H_i^R\right] & \cdot & [0] \\ \cdot & \cdot & \cdot & \cdot & \cdot \\ [0] & \cdot & [0] & \cdot & \left[H_I^R\right] \end{bmatrix},$$

$$\left[T^G\right] = \begin{bmatrix} \left[T_{o1}^G\right] & \cdot & [0] & \cdot & [0] \\ \cdot & \cdot & \cdot & \cdot & \cdot \\ [0] & \cdot & \left[T_{oi}^G\right] & \cdot & [0] \\ \cdot & \cdot & \cdot & \cdot & \cdot \\ [0] & \cdot & [0] & \cdot & \left[T_{oI}^G\right] \end{bmatrix}, \qquad [C] = \begin{bmatrix} [C_1] \\ \cdot \\ [C_i] \\ \cdot \\ [C_I] \end{bmatrix}$$

Matrices $[H_i^R]$, $[T_{oi}^G]$, $[C_i]$ and $[0]$ are square sub-matrices. The total scattered electric and magnetic field from all cylinders, can be easy obtained from

$$\left[E_z^{SGT}\right] = [I]\cdot\left[E_z^{SG}\right] \tag{19}$$

$$\left[H_\phi^{SGT}\right] = [I]\cdot\left[H_\phi^{SG}\right] \tag{20}$$

where matrix $[I]$ consists of diagonal sub-matrices $[I_i] = diag(1)_{-M}^{M}$ as shown $[I] = [[I_1] \dots [I_i] \dots [I_I]]$.

Now the total field on the surface of the interaction region can be defined as

$$[E_z^T] = [E_z^{inc(0)}] + [E_z^{SGT}] \tag{21}$$

$$[H_\phi^T] = [H_\phi^{inc(0)}] + [H_\phi^{SGT}] \tag{22}$$

where $[E_z^{inc(0)}]$ and $[H_\phi^{inc(0)}]$ are diagonal matrices based on (1). To eliminate unknown coefficients (9), a relation between electric and magnetic field on the surface of the interaction region is defined:

$$\left[E_z^T\right] = [Z] \cdot \left[H_\phi^T\right] \tag{23}$$

Hence, the matrix $[Z]$ is given as

$$[Z] = \left(\left[E_z^{inc(0)}\right] + \left[E_z^{SGT}\right]\right) \cdot \left(\left[H_\phi^{inc(0)}\right] + \left[H_\phi^{SGT}\right]\right)^{-1} \tag{24}$$

The formulation of the problem in form of $[Z]$ allows to consider both open and waveguide problems assuming the proper excitations.

2.2. Open Structures

For open problems it is appear to be interesting to describe a total scattered field at any distance ρ from investigating configurations of cylinders. As a source of excitation I plane waves from any ϕ direction (25) are considered. One can assume an excitation, which is located along the negative x-axis at a contour R and can be shifted by an angle θ_{oi} (e.g., see Fig. 6). Total incident and scattered field on our interaction region is defined as

$$E_z^i = \sum_{i=1}^{I} E_{oi} \sum_{n=-\infty}^{\infty} j^{-n} J_n(k_0 R) e^{jn(\phi - \theta_{oi})} \tag{25}$$

$$E_z^s = \sum_{n=-\infty}^{\infty} r_n H_n^{(2)}(k_0 \rho) e^{jn\phi} \tag{26}$$

The corresponding magnetic field along ϕ direction can be established from

$$H_\phi = \frac{1}{j\omega\mu_0} \frac{\partial E_z}{\partial \rho} \tag{27}$$

Orthogonalizing the sets of eigenmode functions of the incident and scattered field (25)–(26) on the surface of cylindrical interaction region

ξ using eigenfunctions $e^{-jm\phi}$ of the field in interaction region and taking into account $n = N$ harmonics the following matrix equations are obtained

$$\begin{aligned}\left[E_z^T\right] &= \left[K^{ET}\right] + \left[K^{ER}\right] \cdot [r] \\ \left[H_\phi^T\right] &= \left[K^{HT}\right] + \left[K^{HR}\right] \cdot [r]\end{aligned} \tag{28}$$

where the n^{th} element of vector

$$[K^{ET}] = \left[\begin{array}{cccccccc} K_{-N}^{ET} & \dots & K_{-1}^{ET} & K_0^{ET} & K_1^{ET} & \dots & K_N^{ET} \end{array}\right]^T$$

has the form $K_n^{ET} = \sum_{i=1}^{I} E_{oi} j^{-n} J_n(k_0\rho_{oi}) e^{-jn\theta_{oi}}$, $[K^{ER}] = diag(H_n^{(2)}(k_0\rho))_{n=-N}^{N}$, $[r] = [r_{-N} \ \dots \ r_{-1} \ r_0 \ r_1 \ \dots \ r_N]^T$ and $[K^{HT}]$, $[K^{HR}]$ formulate vector and square matrix respectively for magnetic field H_ϕ.

Using relation (23) with $[E_z^T]$, $[H_\phi^T]$ defined in (28) and assuming known amplitudes E_{oi} the scattering coefficients r_n can be investigated.

$$[r] = \left(\left[K^{ER}\right] - [Z] \cdot \left[K^{HR}\right]\right)^{-1} \cdot \left([Z] \cdot \left[K^{HT}\right] - \left[K^{ET}\right]\right) \tag{29}$$

Finally, the total scattered field at any distance ρ from interaction region can be obtained from (26). Moreover, the solution for H^z-plane incident wave can be obtained by using the duality principle [15].

2.3. Waveguide Structures

It seems to be interesting to apply the solution (24) in order to combine an equivalent scattered field from cylinders described on the surface of a separated interaction region ξ (contour R) with incident fields from each waveguide's port.

Consider field components of TE_{n0} modes in waveguide port i in its local Cartesian coordinate system (x_i, y_i, z) as follows

$$E_z^i = \sqrt{\frac{2}{a_i b}} \sum_{n=1}^{N_i} \sin\left[\frac{n\pi}{a_i}\left(y_i + \frac{a_i}{2}\right)\right]\left(t_n^i e^{jk_{xn}^i x_i} + r_n^i e^{-jk_{xn}^i x_i}\right) \tag{30}$$

where $k_{xn}^i = \sqrt{\omega^2\varepsilon_0\mu_0 - \left(\frac{n\pi}{a_i}\right)^2}$, $i = 1, 2, \dots, K$ and K denotes number of waveguide ports while magnetic fields can be obtained from $H_x^i = \frac{j}{\omega\mu_0}\frac{\partial}{\partial y_i}E_z^i$, $H_y^i = \frac{1}{j\omega\mu_0}\frac{\partial}{\partial x_i}E_z^i$.

The field components in each port i are rewritten in basic coordinate system (x, y, z) using the following transformation

equations

$$\begin{aligned} x_i &= x\cos\phi_i + y\sin\phi_i \\ y_i &= y\cos\phi_i - x\sin\phi_i \end{aligned} \tag{31}$$

and ϕ_i represents rotation angle between coordinate systems (x, y, z) and (x_i, y_i, z) (see Fig. 3).

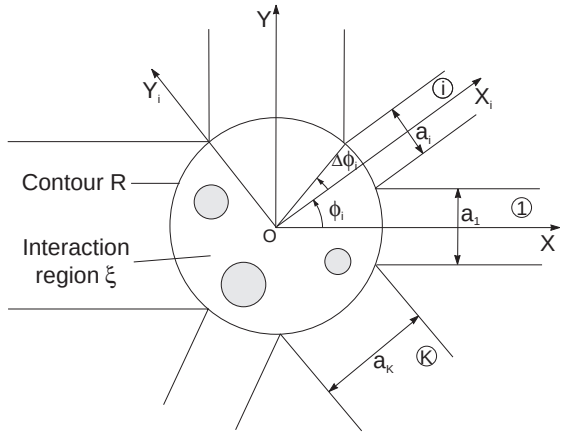

Figure 3. Schematic representation of the investigating structure.

To define the scattering matrix of our investigating structure the continuity conditions between tangential electric and magnetic fields on contour R and fields from waveguide ports described in equation (30) and written in cylindrical coordinates (32) must be satisfied

$$\begin{aligned} E_z &= E_z \\ H_\phi &= -H_x\sin\phi + H_y\cos\phi \end{aligned} \tag{32}$$

for $\rho = R,\ \phi = (0, 2\pi),\ x = R\cos\phi,\ y = R\sin\phi.$

Orthogonalizing the sets of eigenmode functions of the field in each waveguide port using eigenfunctions $e^{-jm\phi}$ of the field in cylindrical interaction region one has

$$\begin{aligned} \left[E_z^T\right] &= \left[K^{ET}\right]\cdot\left[t_1^1 t_2^1 \ldots t_1^i t_2^i \cdots t_1^K t_2^K \ldots\right]^T \\ &\quad + \left[K^{ER}\right]\cdot\left[r_1^1 r_2^1 \ldots r_1^i r_2^i \ldots r_1^K r_2^K \ldots\right]^T \\ \left[H_\phi^T\right] &= \left[K^{HT}\right]\cdot\left[t_1^1 t_2^1 \ldots t_1^i t_2^i \cdots t_1^K t_2^K \ldots\right]^T \\ &\quad + \left[K^{HR}\right]\cdot\left[r_1^1 r_2^1 \ldots r_1^i r_2^i \ldots r_1^K r_2^K \ldots\right]^T \end{aligned} \tag{33}$$

where $[K^{ET}]$, $[K^{ER}]$, $[K^{HT}]$, $[K^{HR}]$ are the square matrices as shown $[K^{AB}] = [[K^{AB_1}] \dots [K^{AB_i}] \dots [K^{AB_K}]]$ for $A = E$ or H and $B = T$ or R. The size of sub-matrix $[K^{AB_i}]$ is $(2M+1)$ by N_i and its elements have the form

$$K_{m,n}^{ET(R)_i} = \sqrt{\frac{2}{a_i b}} \cdot \int_{\phi_i - \Delta\phi_i}^{\phi_i + \Delta\phi_i} e^{-jm\phi} \cdot \sin\left[\frac{n\pi}{a_i}\left(y_i + \frac{a_i}{2}\right)\right] \cdot e^{+(-)jk_{xn}^i x_i} d\phi \tag{34}$$

$$K_{m,n}^{HT(R)_i} = \frac{1}{\omega\mu_0} \cdot \sqrt{\frac{2}{a_i b}} \int_{\phi_i \Delta\phi_i}^{\phi_i + \Delta\phi_i} e^{-jm\phi} \left\{ +(-)k_{xn}^i \cdot \sin\left[\frac{n\pi}{a_i}\left(y_i + \frac{a_i}{2}\right)\right] \cdot \cos\phi \right.$$
$$\left. -j\frac{n\pi}{a_i} \cos\left[\frac{n\pi}{a_i}\left(y_i + \frac{a_i}{2}\right)\right] \cdot \sin\phi \right\} \cdot e^{+(-)jk_{xn}^i x_i} d\phi \tag{35}$$

where $\Delta\phi_i = \arcsin(a_i/2R)$.

In order to obtain quadratic matrices in (33) the number of eigenfunctions in all waveguide ports should equal $K(2M+1)$ where M is the number of eigenfunctions in the cylindrical interaction region and K is the number of ports. As a result, the numbers of eigenfunctions in one of the port should have one more eigenfunction.

Relation between tangential electric and magnetic field of interaction region defined on the contour R (see Fig. 3) can be written as

$$[E_z^T] = [Z] \cdot [H_\phi^T] \tag{36}$$

where the matrix $[Z]$ is given in (24).

Finally, introducing the relation (33) into (36) the modal scattering matrix of the circuit is obtained.

$$[S] = \left(\left[K^{ER}\right] - [Z] \cdot \left[K^{HR}\right]\right)^{-1} \cdot \left([Z] \cdot \left[K^{HT}\right] - \left[K^{ET}\right]\right) \tag{37}$$

3. ESTIMATION OF NUMERICAL ERRORS

In general the number of eigenfunctions and interactions between cylinders should be infinity. For numerical investigation, infinite set of equations, written in matrix form, must be proper truncated. This operation provides to numerical errors which quantities should be estimated both for open and closed structures.

3.1. Open Structures

Plane wave excitation is represented by an infinite sum of cylindrical wave functions as follows

$$E_z = E_o e^{-jk_o x} = E_o e^{-jk_0 R\cos\phi} = E_o \sum_{n=-\infty}^{\infty} j^{-n} J_n(k_0 R) e^{jn\phi} \tag{38}$$

Here, the infinite sum has to be truncated to $n = N$. The choice of the number of harmonics N strongly depends on R. Table 1 shows percentage error for the convergence of plane wave described as sum of cylindrical wave functions for $R = 1\lambda,\ R = 2\lambda,\ R = 3\lambda$ evaluated with the following criterion

$$\delta = \sqrt{\frac{1}{K}\sum_{k=1}^{K} \frac{\left(\left|e^{-jk_0 R\cos\phi_k}\right| - \left|\sum_{n=-N}^{N} j^{-n} J_n(k_0 R) e^{jn\phi_k}\right|\right)^2}{\left|e^{-jk_0 R\cos\phi_k}\right|^2}} \cdot 100\% \tag{39}$$

where ϕ_k represents the angle for which the plane wave electric field is obtained, $\phi_k = 2\pi k/K$ and K is the number of points at the contour R where the field is defined.

Table 1. Comparison of percentage error δ for the convergence of plane wave for different radii R of interaction region and different numbers of harmonics N.

		N	8	9	10	11	12	13	14
$R = 1\lambda$	$K = 360$	δ[%]	3.078	1.08	0.321	0.094	0.023	0.005	0.001
		N	15	16	17	18	19	20	21
$R = 2\lambda$	$K = 360$	δ[%]	2.545	1.09	0.434	0.159	0.056	0.018	0.006
		N	22	23	24	25	26	27	28
$R = 3\lambda$	$K = 360$	δ[%]	1.974	0.917	0.409	0.172	0.068	0.026	0.009

As shown in Table 1, if the radius R of the region ξ is increased, the more harmonic functions are needed to describe excitation with required error δ. From numerical results, it has been observed that further increasing of the value K ($K > 360$ gives angle increment less than 1°) does not change the value of error.

Having established the number of harmonics, it is necessary to obtain the proper number of interactions between cylinders. The root mean square value of the difference between magnitudes of the total scattered tangential field component E_z^s at the distance ρ (see 26) should not exceed 0.1% for P and $P-1$ interaction. Hence, it

is assumed that, in mathematical form, the percentage error can be described as follows

$$\delta_s = \sqrt{\frac{1}{K}\sum_{k=1}^{K} \frac{\left(\left|E_z^{s(P)}(\phi_k)\right| - \left|E_z^{s(P-1)}(\phi_k)\right|\right)^2}{\left|E_z^{s(P)}(\phi_k)\right|^2}} \cdot 100\% \qquad (40)$$

where ϕ_k represents the angle for which the scattered electric field is calculated and $\phi_k = 2\pi k/K$ and K is the number of points where the field is defined. The smallest ϕ_k is, the more accurate representation of the error can be established. Table 2 shows comparison of percentage error δ_s for configuration of cylinders from Fig. 4 for different numbers of points K and different numbers of interactions between cylinders P. For presented configuration one can use $P = 16$ and $K = 720$ to obtain scattered field with an error less than 0.1%.

Table 2. Comparison of percentage error δ_s for configuration of cylinders from Fig. 4 for different numbers of points K and different numbers of interactions between cylinders P ($R = 2\lambda,\ \rho = 100\lambda,\ N = 19$).

	P	10	11	12	13	14	15	16	17
$K = 360$	δ_s [%]	1.078	0.463	0.319	0.275	0.172	0.109	0.083	0.055
$K = 720$	δ_s [%]	1.095	0.499	0.372	0.322	0.192	0.109	0.078	0.051
$K = 1440$	δ_s [%]	1.1202	0.5198	0.3856	0.333	0.197	0.108	0.076	0.049
$K = 3600$	δ_s [%]	1.1222	0.521	0.386	0.333	0.198	0.108	0.076	0.049

It is important to point out that the choice of P strongly depends on the posts configuration. Table 3 presents comparison of percentage error δ_s and the computation times (MATLAB, 800 MHz Pentium III PC) for configurations of cylinders from Figs. 6a, 6b, 7a and 7b for different numbers of interactions P between cylinders. Significant difference can be observed for these two configurations and different angles of excitations. For Fig. 6b one need about 30 interactions between cylinders to obtain error on the level less than 0.1% while for the same level of error, configuration from Fig. 7b, needs about 13 interactions.

Taking into account a lot of numerical investigations, it can be assumed that $K = 720$ and $P > 30$ protects in most of configurations $\delta_s < 0.1\%$.

Table 3. Comparison of percentage error δ_s and the computation times for configurations of cylinders from Figs. 6a, 6b, 7a and 7b for different numbers of interactions between cylinders P ($R = 2\lambda,\ \rho = 100\lambda,\ N = M = 19,\ K = 720$).

	P	10	15	20	30	40	50
Fig. 6a	δ_s [%]	4.896	1.158	0.277	0.026	0.002	< 0.001
	Time [s]	3.79	4.01	4.28	4.89	5.28	5.99
Fig. 6b	δ_s [%]	23.744	9.412	1.694	0.102	0.01	0.001
	Time [s]	3.73	4.01	4.31	4.83	5.27	5.93
	P	3	5	7	9	11	13
Fig. 7a	δ_s [%]	2.599	0.203	0.019	0.003	0.001	< 0.001
	Time [s]	2.47	2.59	2.64	2.69	2.74	2.86
Fig. 7b	δ_s [%]	14.818	6.098	1.423	0.377	0.135	0.031
	Time [s]	2.47	2.58	2.64	2.69	2.75	2.91

3.2. Waveguide Structures

To evaluate the accuracy of the scattering coefficients of TE_{10}-mode for waveguide structure and select the proper number of harmonics N_1, the following error criterions are used.

$$\delta_{S11} = \frac{\left|S_{11}^{N_1}\right| - \left|S_{11}^{N_1-1}\right|}{\left|S_{11}^{N_1}\right|} \cdot 100\%, \quad \delta_{S21} = \frac{\left|S_{21}^{N_1}\right| - \left|S_{21}^{N_1-1}\right|}{\left|S_{21}^{N_1}\right|} \cdot 100\%,$$

$$\Delta = \frac{1 - \left(\left|S_{11}^{N_1}\right| + \left|S_{21}^{N_1}\right|\right)^2}{1} \cdot 100\%, \tag{41}$$

Table 4 shows the comparison of percentage errors δ_{S11}, δ_{S21} and Δ for configurations of lossless cylinders from Fig. 11 for different numbers of harmonics N_1 and interactions P. The proper number of harmonics N_1 can be chosen, by controlling the values of errors δ_{S11}, δ_{S21} at the required level. It is important to notice that error δ_{S21} significantly increases near resonant frequencies, which is due to changes at the low level of signal. The error Δ helps to evaluate the sufficient number of interactions between cylinders P. For small values of $P (P < 10)$ it is seen that energetic condition $(|S11|^2 + |S21|^2 = 1)$ is not satisfied despite the lossless structure. From the physical interpretation of scattering phenomena one can suppose that when the numbers of interactions P is not sufficient then the part of energy has been stored inside the region ξ. With increasing the number

Table 4. Comparison of percentage errors δ_{S11}, δ_{S21} for configurations of cylinders from Fig. 11 ($f/f_c = 1.7$, $\tan\delta_1 = \tan\delta_2 = 0$) for different numbers of harmonics N_1 and different numbers of interactions between cylinders P.

	N_1	9	10	11	12	13	14	15	16
$P = 3$	δ_{S11} [%]	-1.6178	-1.1863	-0.7397	-0.5314	-0.3470	-0.2462	-0.1644	-0.1158
	δ_{S21} [%]	2.4447	1.7483	1.0219	0.7306	0.4617	0.3281	0.2151	0.1521
	Δ [%]	16.3310	16.2400	16.2019	16.1625	16.1420	16.1241	16.1137	16.1053
$P = 5$	δ_{S11} [%]	-1.6995	-1.2673	-0.7816	-0.5668	-0.3678	-0.2625	-0.1745	-0.1234
	δ_{S21} [%]	2.4142	1.6991	1.0008	0.7087	0.4502	0.3180	0.2093	0.1474
	Δ [%]	3.0231	3.0027	2.9942	2.9854	2.9808	2.9769	2.9745	2.9727
$P = 10$	δ_{S11} [%]	-1.7149	-1.2833	-0.7896	-0.5737	-0.3718	-0.2656	-0.1765	-0.1249
	δ_{S21} [%]	2.3970	1.6806	0.9919	0.7008	0.4458	0.3144	0.2071	0.1457
	Δ [%]	0.0027	0.0022	0.0020	0.0019	0.0018	0.0017	0.0017	0.0016
$P = 20$	δ_{S11} [%]	-1.7152	-1.2834	-0.7898	-0.5738	-0.3719	-0.2657	-0.1765	-0.1249
	δ_{S21} [%]	2.3966	1.6804	0.9918	0.7007	0.4457	0.3144	0.2071	0.1457
	Δ [%]	-0.0001	-0.0001	0.0000	0.0000	0.0000	0.0000	0.0000	0.0000

Table 5. Comparison of the second resonance frequency for configurations of cylinders from Fig. 11 ($\tan\delta_1 = \tan\delta_2 = 0$, $P = 30$) for different numbers of harmonics N_1.

N_1	9	10	11	12	13	14	15	16
f_{r2} [GHz]	11.678	11.691	11.698	11.703	11.707	11.709	11.711	11.712
δ_{fr2} [%]	0.290	0.179	0.120	0.077	0.043	0.026	0.009	0.000

of interactions the energy becomes lower because it is passed to the scattered field. For lossy structures the condition $|S11|^2 + |S21|^2 < 1$ so the value of Δ will be stabilized at the level $\Delta > 0$ (e.g., for Fig. 11, $\Delta = 0.22\%$). In presented examples f_c denotes cutoff frequency of the TE_{10} mode for rectangular waveguide.

From Table 5 one can notice that for $N_1 = 13$ it is possible to obtain the resonant frequency with the error $\delta_{fr2} = 0.043\%$ which gives 50 MHz difference in relative to $f_{r2}(N_1 = 16)$.

Taking into account a lot of numerical investigations, the following number of eigenfunctions: interaction region: $M = 13$, waveguide regions: $N_1 = 13$, $N_2 = 14$ is sufficient to obtain $\delta_{S21} < 1\%$ for signal $|S21| \geq -10\,\mathrm{dB}$. Numerical investigations also proved that the sufficient number of P changes for different configurations and numbers of cylinders. Hence, the number of P should be chosen individually in dependence on configuration of the considered junction.

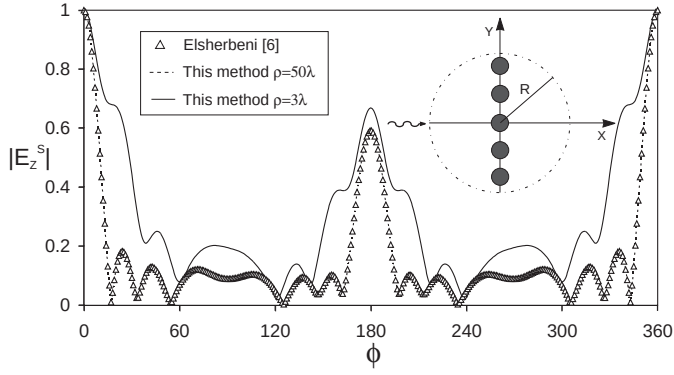

Figure 4. Scattering by an array of 5 identical metallic cylinders located along y-axis. Plane wave excitation in x-axis direction, posts configuration and parameters are described in text ($R = 2\lambda$, $P = 16$, $\delta_s < 0.1\%$, $M = N = 19$, CPU time = 4.07 s).

4. NUMERICAL RESULTS AND DISCUSSION

4.1. Open Structures

A few known examples have been chosen from the literature to test the validity of the method. Fig. 4 shows scattering by a linear array of five metallic cylinders of equal radii ($r = 0.1\lambda$) along y-axis in near area $\rho = 3\lambda$ and at a distance $\rho = 50\lambda$ where λ is the length of the wave in free space. The separation distance between the centers of the cylinders is 0.75λ. For the distance $\rho = 50\lambda$ results agree very well with those obtained by Elsherbeni *et al.* [6].

Fig. 5 presents comparison of scattered field from dielectric cylinders described in Fig. 6 and calculated for different distance ρ from the origin. One can observe that for $\rho > 15\lambda$ the pattern of the scattered field has been stabilized. Numerical investigation allowed to assume that the distance $\rho > 50\lambda$ can be treated in this case as far zone.

The following problem where dielectric posts ($\varepsilon_r = 5$) are excited by E^z-plane wave from different angle of excitation has been described in Figs. 6 and 7. The radius of the center post is 0.15λ while the radii of the rest posts equal 0.1 and are at a distance of 1.5λ from the origin. The radius of interaction region is $R = 2\lambda$. The second structure has been obtained by removing the center post. Comparing Figs. 6 and 7 it is noticeable that presence of the center post strongly indicates the direction of the incident wave.

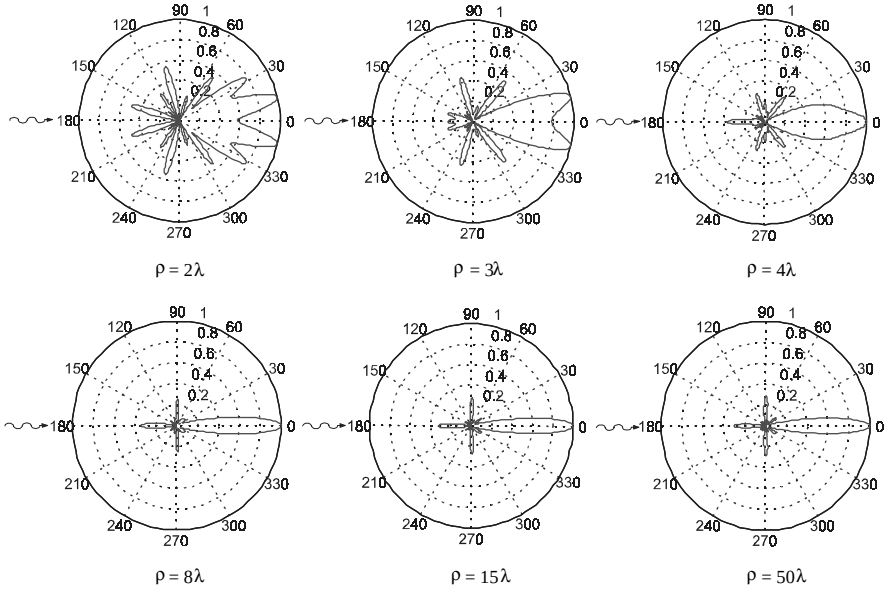

Figure 5. Normalized energy characteristics for scattering by an array of 5 dielectric cylinders (see Fig. 6) for different distance ρ from the origin. Plane wave excitation for $\theta_{O1} = 0°$ ($R = 2\lambda,\ P = 30, \delta_s < 0.1\%,\ M = N = 19$, CPU time = 4.89 s).

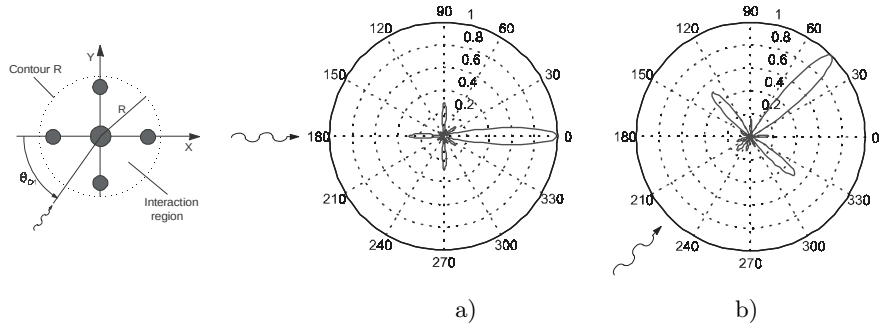

Figure 6. Normalized energy characteristics for scattering by an array of 5 dielectric cylinders for different angle of excitation: a) $\theta_{O1} = 0°$, b) $\theta_{O1} = 45°$ ($R = 2\lambda,\ \rho = 100\lambda,\ P = 30, \delta_s < 0.1\%,\ M = N = 19$, CPU time = 4.89 s).

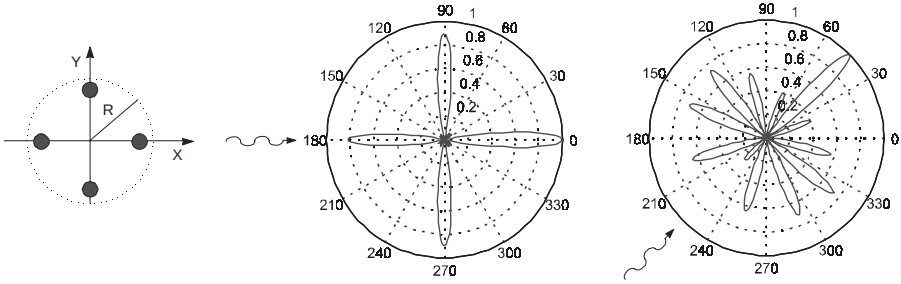

Figure 7. Normalized energy characteristics for scattering by a structure shown in Fig. 6 after removing center post for different angle of excitation: a) $\theta_{O1} = 0°$, b) $\theta_{O1} = 45°$ ($R = 2\lambda$, $\rho = 100\lambda$, $P = 13$, $\delta_s < 0.1\%$, $M = N = 19$, CPU time = 3.18 s).

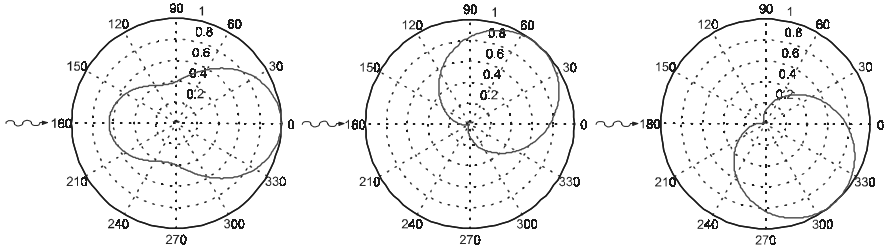

Figure 8. Normalized energy characteristics for scattering from one ferrite cylinder. Plane wave excitation in x-axis direction $\theta_{O1} = 0°$. Ferrite post parameters: $r = 2.6\,\text{mm}$, $\varepsilon_f = 15$, $M_s = 218\,\text{kA/m}$, $H_i = 0$, $f = 10\,\text{GHz}$, $R = 1\lambda$, $\rho = 100\lambda$, $M = N = 13$, CPU time = 0.73 s. a) dielectric cylinder $\varepsilon = \varepsilon_f$, b) ferrite cylinder $M_s = 218\,\text{kA/m}$, c) ferrite cylinder $M_s = -218\,\text{kA/m}$.

Fig. 8 shows calculated far field ($\rho = 100\lambda$) patterns for one cylinder. The radius of cylinder ($r = 2.6\,\text{mm}$) is similar to radii of cylinders used in ferrite circulators for X band. Scattering properties of dielectric (Fig. 8a) and ferrite post (Fig. 8b and 8c) have been compared. For dielectric cylinder symmetric characteristic is observed with respect of plane of excitation. When dielectric is replaced by magnetized ferrite post, squinting characteristic from the direction of excitation is noticed. Squinting effect makes the structure to concentrate energy along $\pm 48°$ direction for opposite magnetization.

Fig. 9 presents normalized energy characteristics for scattering

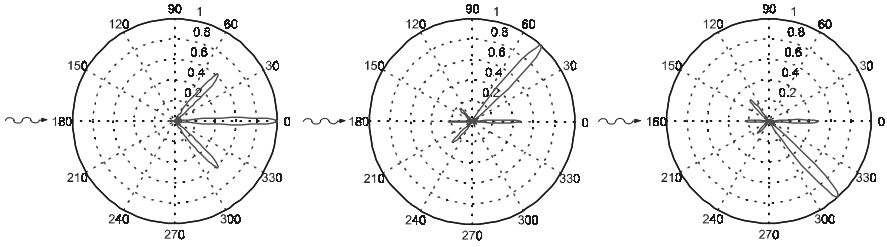

Figure 9. Normalized energy characteristics for scattering from configuration of five ferrite cylinders located along y-axis. Plane wave excitation in x-axis direction $\theta_{O1} = 0^\circ$. Ferrite posts parameters: $r = 4.8\,\mathrm{mm}$, $\varepsilon_f = 5$, $M_s = 348.8\,\mathrm{kA/m}$, $H_i = 0$, $f = 10\,\mathrm{GHz}$, $R = 3\lambda$, $\rho = 100\lambda$, $P = 40$, $\delta_s < 0.1\%$, $M = N = 26$, CPU time $= 10.23\,\mathrm{s}$. a) dielectric cylinder $\varepsilon = \varepsilon_f$, b) ferrite cylinder $M_s = 348.8\,\mathrm{kA/m}$, c) ferrite cylinder $M_s = -348.8\,\mathrm{kA/m}$.

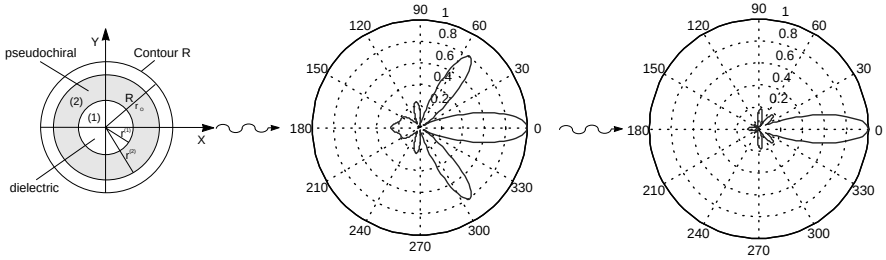

Figure 10. Normalized energy characteristics for scattering from one pseudochiral cylinder. Plane wave excitation for $\theta_{O1} = 0^\circ$. Dimensions: $r^{(1)} = 0.4\lambda$, $r^{(2)} = 0.8\lambda$, $R = 1\lambda$, $\rho = 100\lambda$, $M = N = 13$, CPU time $= 0.84\,\mathrm{s}$. a) dielectric cylinder: layer (1) $\varepsilon^{(1)} = 1$, layer (2), (host medium) $\varepsilon^{(2)} = 4$, $\varepsilon_z^{(2)} = 4$, b) pseudochiral cylinder: layer (1) $\varepsilon^{(1)} = 1$, layer (2) $\varepsilon^{(2)} = 4$, $\varepsilon_z^{(2)} = 9$, $\mu^{(2)} = 1$, $\mu_\rho^{(2)} = 1.5$.

from linear array of five ferrite cylinders of equal radii ($r = 4.8\,\mathrm{mm}$) along y-axis at a distance $\rho = 100\lambda$ (see configuration in Fig. 4). The separation distance between the centers of the cylinders is 1.35λ. Similar squinting properties like in Fig. 8 are observed, but the main beam narrows significantly. This effect strongly depends on the distance between cylinders.

It seems to be interesting to notice that different phenomena decide about squinting properties of examined structures. In the case of one ferrite cylinder $\mu_{eff} > 0$ and resonance effect occurs in post. For configuration of five ferrite cylinders $\mu_{eff} < 0$ and we can suppose that squinting properties depends on field displacement effect.

Numerical experiments have also been carried out for pseudochiral cylinder. Considering Fig. 10 one can observe that the level of side lobes of the pseudochiral cylinder characteristic (Fig. 10b) in comparison with the one of dielectric cylinder (Fig. 10a) decreases significantly.

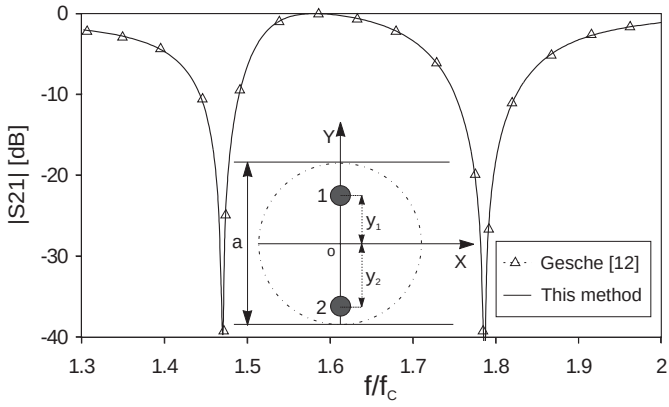

Figure 11. S_{21} parameter for a two dielectric cylinders located in a rectangular waveguide versus f/f_c : $r_1 = r_2 = 0.03 \cdot a$, $\varepsilon_1 = \varepsilon_2 = 38.5$, $\tan\delta_1 = \tan\delta_2 = 2 \cdot 10^{-4}$, $x_1 = 0$, $y_1 = 0.3 \cdot a$, $x_2 = 0$, $y_2 = -0.425 \cdot a$, where a denotes waveguide width and r_1, r_2 is the radius of the cylinder 1 and 2 respectively ($N_1 = 13$, $N_2 = 14$, $M = 13$, $P = 30$).

4.2. Waveguide Structures

Scattering parameters are compared with results obtained by Gesche and Löchel [12] (see Fig. 11) and practically no difference can be observed. Other configurations of posts from [9] and [13] have also been tested and results give very good agreement.

Fig. 12 shows frequency responses for two configurations of three posts located in a rectangular waveguide. The first configuration is presented in Fig. 12 while second one has been obtained after rotation all the structure by an angle $\phi_O = 45°$. With rotation the tuning of the resonance frequencies is observed.

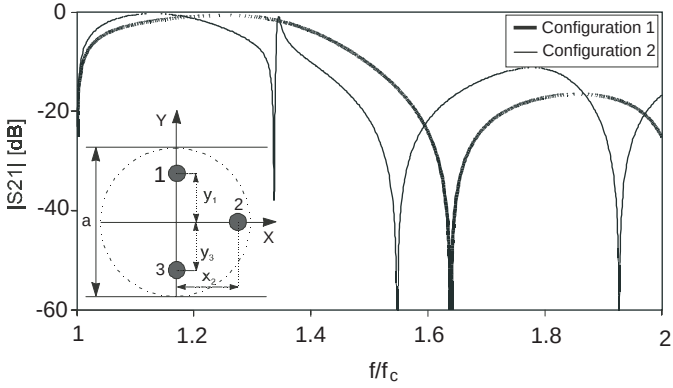

Figure 12. S_{21} parameter for a set of three cylindrical dielectric posts located in a rectangular waveguide versus f/f_c. ($N_1 = 13,\ N_2 = 14,\ M = 13,\ P = 55$). Configuration 1: $r_1 = r_2 = r_3 = 0.03 \cdot a,\ \varepsilon_1 = \varepsilon_2 = \varepsilon_3 = 38.5,\ \tan\delta_1 = \tan\delta_2 = 2 \cdot 10^{-4},\ x_1 = 0,\ y_1 = 0.35 \cdot a,\ x_2 = 0.375 \cdot a,\ y_2 = 0,\ x_3 = 0,\ y_3 = -0.35 \cdot a$, where a denotes waveguide width. Configuration 2: structure rotated by an angle $\phi_O = 45°$.

Numerical experiments have also been carried out for 4-port waveguide junction containing two ferrite cylinders inserted in bi-directional magnetic field along z axis (see Fig. 13). In addition, posts have been placed in dielectric ($\varepsilon_r = 4.8$) and this structure represents interaction region ξ in investigated junction. The purpose of this procedure was reduction of the reflection coefficients. Considering the first configuration (Fig. 13a), transmission from port 1 to port 2 is observed. When directions of magnetized fields are reversed, input signal from port 1 is divided equally between ports 3 and 4 (Fig. 13b) and slightly signal appears in port 2.

The transmission frequency characteristics of a rectangular waveguides with two-layered dielectric and pseudochiral cylinder are respectively presented in Figs. 14a and 14b. It is evident that the pseudochirality effect had the influence on the shift of resonance frequency.

Finally, it is worth mentioning that presented method is fast and easy to implement on personal computer. For open problems execution time in MATLAB on an 800 MHz Pentium III PC for one cylinder was about 1 s ($M = 13$) and 5 s ($M = 19$) for five cylinders. For closed problems numerical aspects of S matrix computations are collected in Table 6, which shows the number of eigenfunctions in the cylindrical interaction region and the computation times in MATLAB on an 800 MHz Pentium III PC for one, two and three cylinders in 2-port

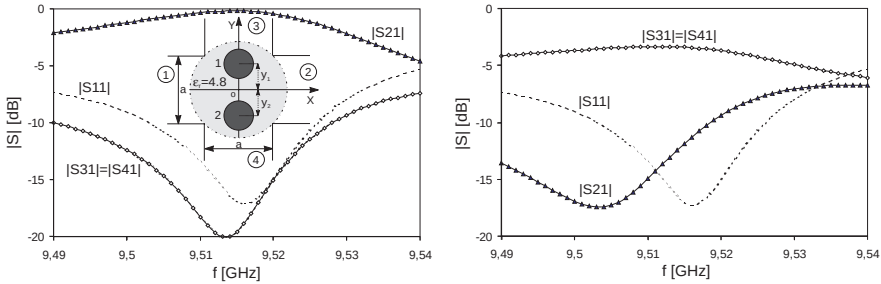

Figure 13. Frequency dependent S-characteristics of the 4-port waveguide junction containing two ferrite posts in dielectric cylinder: $N_1 = 14,\ N_2 = N_3 = N_4 = 13,\ M = 26,\ P = 30,\ r_1 = r_2 = 4.7\,\text{mm},\ \varepsilon_1 = \varepsilon_2 = 16.3,\ \varepsilon_r = 4.8,\ x_1 = 0,\ y_1 = 0.38 \cdot a,\ x_2 = 0,\ y_2 = -0.38 \cdot a$, a) $M_{s1} = 218\,\text{kA/m},\ M_{s2} = -218\,\text{kA/m},\ H_{i1} = 73.21\,\text{kA/m},\ H_{i2} = -73.21\,\text{kA/m}$, b) $M_{s1} = -218\,\text{kA/m},\ M_{s2} = 218\,\text{kA/m},\ H_{i1} = -73.21\,\text{kA/m},\ H_{i2} = 73.21\,\text{kA/m}$.

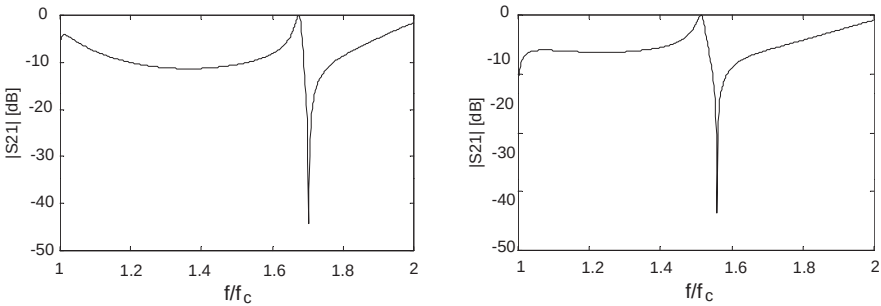

(a) (b)

Figure 14. Transmission characteristics S_{21} versus f/fc of a rectangular waveguide lossless dielectric (a) and psedochiral (b) cylinder located at $x_1 = 0,\ y_1 = 0,\ N_1 = 13,\ N_2 = 14,\ M = 13$. Dimensions of the cylinder (see Fig. A1) $r^{(1)} = 0.05 \cdot a,\ r^{(2)} = 0.16 \cdot a$, where a denotes waveguide width. Material parameters: a) dielectric cylinder $\varepsilon^{(1)} = 1,\ \varepsilon^{(2)} = 20$, b) pseudochiral cylinder $\varepsilon^{(1)} = 1,\ \varepsilon_z^{(2)} = 20,\ \mu = 1,\ \mu_\rho^{(2)} = 1.5$.

Table 6. S matrix computation time in seconds.

2-port junction				4-port junction			
	One post	Two posts	Three posts		One post	Two posts	Three posts
M	$P = 1$	$P = 30$	$P = 60$	M	$P = 1$	$P = 30$	$P = 60$
11	0.22 s	0.38 s	0.88 s	22	0.71 s	1.37 s	3.18 s
13	0.27 s	0.49 s	1.21 s	26	0.88 s	1.92 s	4.61 s
15	0.33 s	0.66 s	1.48 s	30	1.09 s	2.53 s	6.32 s

waveguide junction (dielectric posts) and 4-port waveguide junction (ferrite posts).

5. CONCLUSION

The analysis for E^z-wave scattering by an array of conducting, lossy dielectric, ferrite and/or psudochiral cylinders has been developed using a combination of modified iterative scattering procedure and the orthogonal expansion method. This approach is convenient for investigations of the open and waveguide problems. Presented method is fast, accurate and allows to simulate different structures, which can be interesting in microwave design. The validity and accuracy of the method has been verified by comparing the numerical results with those given in literature. The analysis given above allowed to investigate number of novel structures.

For open structures, interesting effects of changing characteristics have been noticed for different configurations of dielectric cylinders. For ferrite posts squinting characteristic from the direction of excitation has been shown. One pseudochiral cylinder has been analysed and the reduction of the level of side lobes has been observed in comparison to the dielectric one. Presented approach is convenient to describe a total scattered field at any distance from investigating configurations of cylinders.

The usefulness of the presented approach have been performed by investigation of the waveguide structures. The tuning of the resonance frequencies has been observed with the rotation of the cylinders configuration located in rectangular waveguide. Waveguide 4-port junction containing two ferrite cylinders inserted in bi-directional magnetic field has been investigated showing its switching properties.

APPENDIX A.

Description of cylindrical E^z-wave in the post made of following materials.

A.1. Dielectric

$$\begin{aligned} \vec{D} &= \varepsilon_0 \varepsilon_r \vec{E} \\ \vec{B} &= \mu_0 \mu_r \vec{H} \end{aligned} \tag{A1}$$

where ε_r, μ_r are scalars.

$$\rho \frac{\partial}{\partial \rho} \left(\rho \frac{\partial E_z}{\partial \rho} \right) + k_0^2 \varepsilon_r \mu_r \rho^2 E_z + \frac{\partial^2 E_z}{\partial \varphi^2} = 0 \tag{A2}$$

The solution of wave Equation (A2) is given by

$$E_z = \sum_{m=-M}^{M} a_m J_m(k\rho) e^{jm\phi} \tag{A3}$$

The magnetic field along ϕ direction can be obtained from

$$H_\phi = \frac{1}{j\omega\mu_0} \frac{\partial E_z}{\partial \rho} \tag{A4}$$

$[G]$ matrix in (7) has the following form

$$[G] = diag \left(\frac{J_m(kr) J_m'(k_0 r) - \sqrt{\dfrac{\varepsilon_r}{\varepsilon_0}} J_m'(kr) J_m(k_0 r)}{\sqrt{\dfrac{\varepsilon_r}{\varepsilon_0}} J_m'(kr) H_m^{(2)}(k_0 r) - J_m(kr) H_m^{(2)'}(k_0 r)} \right)_{m=-M}^{M} \tag{A5}$$

where $k = k_0 \sqrt{\varepsilon_r}$, ε_r is relative electric permittivity and for metallic cylinder we assume $\varepsilon_r = -j\infty$.

A.2. Ferrite

For ferrite cylinder magnetized along z direction material equations are defined as [16]

$$\begin{aligned} \vec{D} &= \varepsilon_0 \varepsilon_f \vec{E} \\ \vec{B} &= \mu_0 \overleftrightarrow{\mu} \vec{H} \end{aligned} \tag{A6}$$

where ε_f is a scalar and $\overleftrightarrow{\mu}$ have the following dyadic form as

$$\overleftrightarrow{\mu} = \mu \left(\vec{a}_\rho \vec{a}_\rho + \vec{a}_\phi \vec{a}_\phi \right) + j\mu_a \left(\vec{a}_\phi \vec{a}_\phi - \vec{a}_\rho \vec{a}_\rho \right) + 1 \cdot \vec{a}_z \vec{a}_z \tag{A7}$$

The wave equation is given by

$$\rho\frac{\partial}{\partial\rho}\left(\rho\frac{\partial E_z}{\partial\rho}\right)+k_0^2\varepsilon_f\mu_{eff}\rho^2E_z+\frac{\partial^2E_z}{\partial\varphi^2}=0 \tag{A8}$$

The solution of wave Equation (A8) has the form

$$E_z=\sum_{m=-M}^{M}a_mJ_m(k\rho)e^{jm\phi} \tag{A9}$$

and magnetic field component H_ϕ is written as

$$H_\phi=\frac{1}{j\omega\mu_0\mu_{eff(i)}}\left(\frac{\partial E_z}{\partial\rho}+j\frac{\mu_a}{\mu\rho}\frac{\partial E_z}{\partial\phi}\right) \tag{A10}$$

The matrix $[G]$ is defined as

$$[G]=diag\left(\frac{k_0J_m(kr)J_m'(k_0r)-J_m(k_0r)\left[\frac{k}{\mu_{eff}}J_m'(kr)-m\frac{\mu_a}{\mu_{eff}\mu r}J_m(kr)\right]}{H_m^{(2)}(k_0r)\left[\frac{k}{\mu_{eff}}J_m'(kr)-m\frac{\mu_a}{\mu_{eff}\mu r}J_m(kr)\right]-k_0J_m(kr)H_m^{(2)'}(k_0r)}\right)_{m=-M}^{M} \tag{A11}$$

where $k=\omega\sqrt{\varepsilon_f\mu_{eff}}$, ε_f-relative ferrite permittivity and $\mu_{eff}=(\mu^2-\mu_a^2)/\mu$ denotes effective ferrite permeability where μ, μ_a are tensor elements.

For $\mu_a=0$ and $\mu_{eff}=\mu=1$ (dielectric structure) Equation (A5) is obtained.

A.3. Pseudochiral

Constitutive equations for structure described in Fig. A1 are as follows [17, 18]

$$\begin{aligned}\vec{D}&=\varepsilon_0\vec{\vec{\varepsilon}}\,\vec{E}+j\underline{\Omega}_{z\rho}\vec{B}_\rho\\ \vec{B}&=\mu_0\vec{\vec{\mu}}\vec{H}-j\mu_0\vec{\vec{\mu}}\underline{\Omega}_{\rho z}\vec{E}_z\end{aligned} \tag{A12}$$

where $\vec{\vec{\varepsilon}}$, $\vec{\vec{\mu}}$ and $\underline{\Omega}$ are given in dyadic forms as

$$\begin{aligned}\vec{\vec{\varepsilon}}&=\varepsilon\vec{a}_\rho\vec{a}_\rho+\varepsilon\vec{a}_\phi\vec{a}_\phi+\varepsilon_z\vec{a}_z\vec{a}_z\\ \vec{\vec{\mu}}&=\mu_\rho\vec{a}_\rho\vec{a}_\rho+\mu\vec{a}_\phi\vec{a}_\phi+\mu\vec{a}_z\vec{a}_z\end{aligned} \tag{A13}$$

and

$$\begin{aligned}\underline{\Omega}_{z\rho}&=\Omega\vec{a}_z\vec{a}_\rho\\ \underline{\Omega}_{\rho z}&=\Omega\vec{a}_\rho\vec{a}_z\end{aligned} \tag{A14}$$

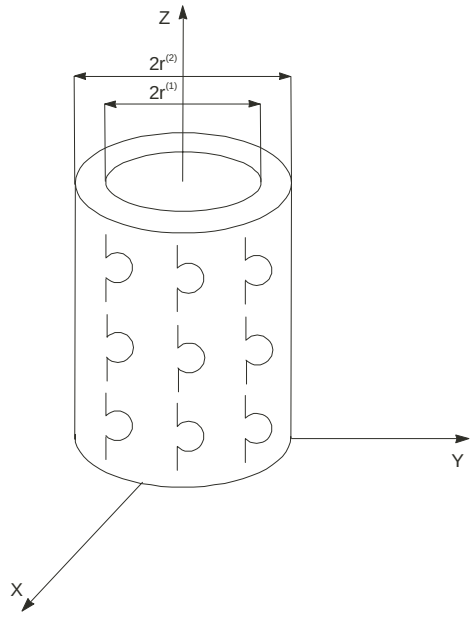

Figure A1. Psudochiral cylinder geometry.

Ω denotes pseudochiral admittance, $\varepsilon_z > \varepsilon$, $\mu_\rho > \mu$ and ε, μ are the parameters of a host medium where ε_z, μ_ρ depend on Ω. For $\Omega = 0$, $\varepsilon_z \to \varepsilon$ and $\mu_\rho \to \mu$.

For configuration from Fig. A1, the following wave equation is obtained

$$\rho \frac{\partial}{\partial \rho}\left(\rho \frac{\partial E_z}{\partial \rho}\right) + k_0^2 \varepsilon_z \mu \rho^2 E_z + \frac{\mu}{\mu_\rho}\frac{\partial^2 E_z}{\partial \varphi^2} = 0 \tag{A15}$$

It is important to note that the element $\varepsilon_z \neq \varepsilon$ and $\mu_\rho \neq \mu$ indicate the pseudichirality effect in the considered cylinder. The solution of wave Equation (A15) is

$$E_z = \sum_{m=-M}^{M} \left(a_m J_v(k\rho) + d_m Y_v(k\rho)\right) e^{jm\phi} \tag{A16}$$

where $v = m\sqrt{\mu/\mu_\rho}$ and magnetic field component H_ϕ can be established from

$$H_\phi = \frac{1}{j\omega\mu_0\mu}\frac{\partial E_z}{\partial \rho} \tag{A17}$$

Solution of Equation (A15) requires noninteger values v of order of Bessel functions defining the field inside the pseudochiral cylinder. To

take into account practical applications, we cover with the pseudochiral material the inner core, which can be dielectric or metallic. Presented considerations provide to minimum two-layered cylindrical structure with external pseudochiral layer, which gives the following matrix $[G]$

$$[G] = diag\left(\frac{J_m\left(k_0 r^{(2)}\right)\cdot X'_v - k_0 J'_m\left(k_0 r^{(2)}\right)\cdot X_v}{k_0 H_m^{(2)'}\left(k_0 r^{(2)}\right)\cdot X_v - H_m^{(2)}\left(k_0 r^{(2)}\right)\cdot X'_v}\right)_{m=-M}^{M} \tag{A18}$$

where

$$\begin{aligned} X_v &= J_v\left(k^{(2)} r^{(2)}\right) + A_v \cdot Y_v\left(k^{(2)} r^{(2)}\right), \\ X'_v &= k^{(2)} J'_v\left(k^{(2)} r^{(2)}\right) + A_v \cdot k^{(2)} Y'_v\left(k^{(2)} r^{(2)}\right) \end{aligned}$$

and A_v has the following form for dielectric and metallic inner core respectively

$$\begin{aligned} A_v &= \frac{k^{(1)} J_v\left(k^{(2)} r^{(1)}\right) J'_m\left(k^{(1)} r^{(1)}\right) - k^{(2)} J'_v\left(k^{(2)} r^{(1)}\right) J_m\left(k^{(1)} r^{(1)}\right)}{k^{(2)} Y'_v\left(k^{(2)} r^{(1)}\right) J_m\left(k^{(1)} r^{(1)}\right) - k^{(1)} Y_v\left(k^{(2)} r^{(1)}\right) J'_m\left(k^{(1)} r^{(1)}\right)}, \\ A_v &= -\frac{J_v\left(k^{(2)} r^{(1)}\right)}{Y_v\left(k^{(2)} r^{(1)}\right)} \end{aligned}$$

The prime symbol denotes the derivative with respect to argument.

REFERENCES

1. Richmond, J. H., "TE-wave scattering by a dielectric cylinder of arbitrary cross-section shape," *IEEE Trans. Antennas Propagat.,* Vol. AP-14, 460–464, 1966.
2. Jim, J. M. and V. V. Liepa, "Application of hybrid finite element method to electromagnetic scattering from coated cylinders," *IEEE Trans. Antennas Propagat.,* Vol. AP-36, 50–54, 1988.
3. Ragheb, H. A. and M. Hamid, "Scattering by N parallel conducting circular cylinders," *Int. J. Electron.,* Vol. 59, 407–421, 1985.
4. Elsherbeni, A. Z. and M. Hamid, "Scattering by parallel conducting circular cylinders," *IEEE Trans. Antennas Propagat.,* Vol. AP-35, 355–358, 1987.
5. Chew, C. W., L. Gurel, Y. M. Wang, G. Otto, R. L. Wagner, and Q. H. Liu, "A generalized recursive algorithm for wave scattering solution in two dimensions," *IEEE Trans. Microwave Theory Tech.,* Vol. 40, 716–723, April 1992.

6. Elsherbeni, A. Z., M. Hamid, and G. Tian, "Iterative scattering of a Gaussian beam by an array of circular conducting and dielectric cylinders," *J. of Electromagnetic Waves and Appl.,* Vol. 7, No. 10, 1323–1342, 1993.
7. Nielsen, E. D., "Scattering by a cylindrical post of complex permittivity in a waveguide," *IEEE Trans. Microwave Theory Tech.,* Vol. 17, 148–153, 1969.
8. Sahalos, J. N. and E. Vafiadis, "On the narrow-band microwave filter design using a dielectric rod," *IEEE Trans. Microwave Theory Tech.,* Vol. 33, 1165–1171, Nov. 1985.
9. Hsu, C. G. and H. A. Auda, "Multiple dielectric posts in a rectangular waveguide," *IEEE Trans. Microwave Theory Tech.,* Vol. 34, 883–891, Aug. 1986.
10. Ise, K. and M. Koshiba, "Numerical analysis of H-plane waveguide functions by combination of finite and boundary elements," *IEEE Trans. Microwave Theory Tech.,* Vol. 36, 1343–1351, Sep. 1988.
11. Gesche R. and N. Löchel, "Scattering by a lossy dielectric cylinder in a rectangular waveguide," *IEEE Trans. Microwave Theory Tech.,* Vol. 36, 137–144, Jan. 1988.
12. Gesche R. and N. Lochel, "Two cylindrical obstacles in a rectangular waveguide-resonances and filter applications," *IEEE Trans. Microwave Theory Tech.,* Vol. 37, 962–968, June 1989.
13. Valero A. and M. Ferrando, "Full-wave equivalent network representation for multiple arbitrary shaped posts in H-plane waveguide," *IEEE Trans. Microwave Theory Tech.,* Vol. 47, 1997–2002, Oct. 1999.
14. Abramovitz, M. and I. Stegun, *Handbook of Mathematical Functions,* Dover, New York, 1970.
15. Balanis, C. A., *Advanced Engineering Electromagnetics,* Wiley, New York, 1989.
16. Baden Fuller, A. J., *Ferrites at Microwave Frequencies,* Peter Peregrinus, Ltd., 1987.
17. Engheta, N. and M. M. Saadoun, "Novel pseudochiral or Ω-medium and its applications," *Proc. of PIERS'91,* 339, Cambridge, MA, July 1991.
18. Saddoun, M. M., "The pseudochiral Ω-medium: Theory and potential applications," Ph.D. Dissertation, University of Pennsylvania, USA, September 1992.